



Super Convergent Finite Beam Element for Torsional Vibration of Open Thin-Walled Vlasov Beam under Torsional Excitations

Alqasim M. Kamour¹, Mohammed A. Hjadi^{2*}, Hasan M. Nagiar³

^{1,2,3} Applied mechanics division, Department of Mechanical and Industrial Engineering, University of Tripoli, Faculty of Engineering, Tripoli, Libya

عنصر عارضة محدود فائق التقارب للاهتزاز الالتوائي لعارضة فلاسوف ذات مقطع عرضي مفتوح رقيق الجدار تحت الاثارات الالتوائية

قاسم كامور¹، محمد الحجاجي^{2*}، حسن النجار³

^{1,2,3} شعبة الميكانيكا التطبيقية، قسم الهندسة الميكانيكية والصناعية، كلية الهندسية، جامعة طرابلس، طرابلس، ليبيا

*Corresponding author: m.hjadi@uot.edu.ly

Received: February 20, 2025

Accepted: April 16, 2025

Published: April 24, 2025

Abstract

A highly accurate finite beam element is developed for the steady state torsional-warping dynamic analysis of open thin-walled doubly symmetric Vlasov beams subjected to various harmonic torsional and warping moments. The governing dynamic equation and associated boundary conditions for torsional-warping response is derived through Hamilton variational principle. The formulation is based on Vlasov beam theory and incorporates both warping deformation and warping inertia effects. From the resulting torsional equation, the closed form solution is exactly obtained. A set of shape functions developed based on the exact solution of the field torsional equation is utilized to formulate the finite beam element. The two-noded beam element, with four degrees of freedom per element, effectively captures the quasi-static and steady-state torsional responses of open thin-walled doubly symmetric beams under harmonic torsional excitations. Additionally, it is used to extract the natural torsional frequencies and mode-shapes from the steady state dynamic response. The results obtained from the finite-element formulation are evaluated and verified by comparing them with well-established finite-element solutions and exact solutions available in the literature. The present beam element validity is demonstrated through several numerical examples, with results exhibiting excellent agreement with exact solutions available in the literature and Abaqus and Galerkin finite element models, achieved at a significantly reduced computational and modeling cost.

Keywords: Warping deformation, exact shape functions, Torsional response, efficient finite element.

المخلص

طُوّر عنصر عارضة محدود عالي الدقة للاستجابة الديناميكية للالتواء والفتل في الحالة المستقرة لعارضات فلاسوف ذات مقاطع عرضية مفتوحة مزدوجة التماثل ورقيفة الجدار المعرضة لعزوم الالتواء والفتل التوافقية المختلفة. استُنبطت المعادلة لعارضة فلاسوف الديناميكية الحاكمة والشروط الحدية المرتبطة بها لاستجابة الالتواء-الفتل من مبدأ هاملتون للتغير. تستند الصياغة إلى نظرية عارضة فلاسوف، وتراعي آثار تشوه الانحناء وقصوره الذاتي. ومن معادلة الالتواء الناتجة، يُحصل على حل الشكل المغلق بدقة. تُستخدم مجموعة من دوال الشكل، التي طُوّرت بناءً على الحل الدقيق لمعادلة الالتواء، لصياغة عنصر العارضة المحدود. يلتقط عنصر الشعاع ثنائي العقد، بأربع درجات حرية لكل عنصر، بفعالية الاستجابات الالتوائية شبه الساكنة والمستقرة للعارضات المفتوحة ورقيفة الجدار مزدوجة التماثل تحت إثارات الالتواء والفتل التوافقية. بالإضافة

إلى ذلك، يُستخدم لاستخلاص الترددات الالتوائية الطبيعية وأشكال الأنماط من الاستجابة الديناميكية في الحالة المستقرة. تُقِيم النتائج المُستقاة من صياغة العناصر المحدودة وتُتحقق من صحتها بمقارنتها بحلول العناصر المحدودة المُثبتة والحلول الدقيقة المُتاحة في المراجع العلمية. وتُبرهن العديد من الأمثلة العددية على صحة عنصر العارضة الحالي، حيث تُظهر النتائج توافقاً ممتازاً مع الحلول الدقيقة المُتاحة في المراجع العلمية ونماذج العناصر المحدودة Galerkin و Abaqus، وقد تحققت ذلك بتكلفة حسابية ونمذجة مُنخفضة بشكل ملحوظ.

الكلمات المفتاحية: تشوه الفتل، دوال الشكل الدقيق، الاستجابة الالتوائية، العناصر المحدودة الفعالة.

Introduction and Objective

Thin-walled members are widely utilized in the design of various structural components, including aerospace structures, steel buildings, bridges, ship and marine frames, and truck chassis. These beams, when subjected to cyclic harmonic torsional excitations, are susceptible to fatigue failures. Under such loads, the overall torsional response of a thin-walled beam consists of two parts: (a) a transient torsional response, which occurs at the onset of the excitation and diminishes rapidly due to damping, and (b) a steady-state torsional response, which persists over time. While the transient response has minimal significance for fatigue design, the steady-state response is important and serves as the primary focus of this study. This paper aims to develop an exact closed-form solution and efficient finite beam element solution that accurately captures and isolates the steady-state torsional-warping dynamic response of open thin-walled doubly symmetric beams. The proposed finite element solution can account for the quasi-static and steady-state torsional dynamic responses. Furthermore, it is also predicting the torsional eigenfrequencies and eigenmodes of the given thin-walled beams.

Literature Review on Finite Element Solutions

In general, finite element formulations are classified into three categories of shape functions: (1) approximate polynomial interpolation functions, (2) shape functions derived from the exact solution of static equilibrium equations, and (3) shape functions based on the exact solution of dynamic equations of motion. Formulations using approximate shape functions are most common, as seen in the works of [3-5]. Kameswara et al. [3] utilized the finite element method to analyze the torsional vibration of long thin-walled open-section beams on elastic foundations. Chen and Tamma [4] developed a finite element method for analyzing thin-walled open members subjected to constant transverse loads, utilizing assumed linear and cubic displacement shape functions along with an implicit, unconditionally stable integration scheme. Aminbaghai et al. [5] developed a formulation for non-uniform torsion in thin-walled beams, capturing the influence of variable axial force and secondary torsion-moment deformation. Additionally, the transfer matrix method was used to develop a finite beam element for static and dynamic analysis.

Finite element formulations based on the exact solution for static equilibrium equations, as seen in references [6-9] and more recently [10], offer the advantage of avoiding locking issues, which can arise with polynomial interpolation functions. In Mei [6], a finite element was developed for coupled free vibration analysis of thin-walled beams, incorporating warping effects using shape functions derived from static equilibrium solutions. Hu et al. [7] introduced a finite element formulation for coupled bending-torsional dynamic behavior of thin-walled beams with asymmetric cross-sections, using interpolation functions based on static differential equilibrium solutions. Mohareb and Nowzartash [8] developed a finite beam element formulation for torsional analysis of thin-walled beams with open cross-sections, using exact static solutions based on Saint-Venant and Vlasov theories. This approach is grounded in the generalized Timoshenko-Vlasov beam theory. Hjadi and Mohareb [9] introduced a super-convergent finite beam element solution for coupled flexural-torsional analysis of monosymmetric thin-walled open beams under general static forces, incorporating warping stiffness and shear deformation effects. Recently, Hjadi et al. [10] formulated an exact finite beam element solution for the torsional-warping coupled static response of doubly symmetric open thin-walled beams.

For dynamic equations of motion, finite element formulations based on exact solutions include the works of references [11-12]. Hjadi and Mohareb [11] developed a super-convergent two-noded finite beam element for dynamic response analysis of monosymmetric thin-walled I-beams under harmonic flexural and torsional loads, considering the effects of Saint Venant and warping torsion translational and rotary inertia and the coupling between bending and torsion. Hjadi et al. [12] developed a super-convergent finite beam element formulation for the torsional-warping dynamic coupled analysis of thin-walled open doubly symmetric beams under various harmonic torsional and warping moments. Their formulations are based on a generalized Vlasov-Timoshenko beam theory, which accounts for shear deformation effects due to non-uniform warping.

Finite element formulations based on approximate shape functions involve spatial discretization errors and require finer meshes to converge to the correct solution. In contrast, formulations using exact solutions have two key advantages: (1) they eliminate discretization errors inherent in conventional interpolation schemes and converge to the solution with fewer degrees of freedom, and (2) they are free from shear locking. This paper aims to establish the exact closed-form and efficient finite beam element solutions for the torsional dynamic analysis of open thin-

walled Vlasov beams with doubly symmetric cross-sections, subjected to various harmonic torsional and warping moments. The proposed approach employs the exact shape functions that fully satisfy the torsional field equation. Initially, exact closed-form torsional solutions for thin-walled beams under harmonic torsional and warping moments are derived for various boundary conditions. Subsequently, an efficient finite beam element formulation is developed, utilizing these exact shape functions to model torsional and warping deformations.

Kinematic Functions

The geometry and coordinate systems for thin-walled beam with doubly symmetric open section are shown in Figure (1). Two sets of coordinate systems are considered in the present formulation, the first set is the Cartesian coordinate system (X, Y, Z) , where X axis is the beam longitudinal axis while Y, Z axes are the principal axes passing through the section centroid C . The second set is the local coordinate system (s, n, Z) , where coordinates n and s are measured along the normal and tangent to the middle surface at the arbitrary point $p(y, z)$, situated on the mid-surface of the cross-section. The formulation presented here is grounded on the following core assumptions:

1. The thin-walled beam cross-section is open doubly symmetric,
2. The beam is linearly elastic and prismatic,
3. Strains and rotations are assumed to be small,
4. The cross-section is assumed to remain undeformed in its own plane, in accordance with Vlasov's first assumption, Vlasov [1],
5. The steady state torsional response is only pursued.

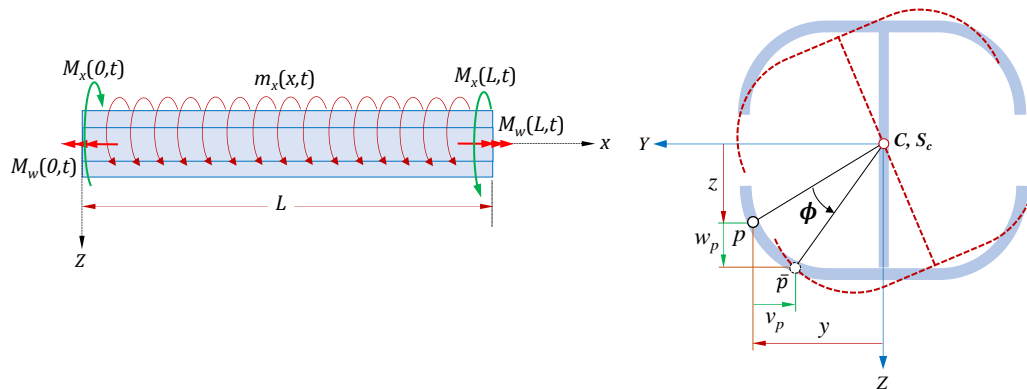


Figure 1: Thin-walled doubly-symmetric beam under various dynamic torsional and warping moments.

Based on the above assumptions and considering that the doubly symmetric open thin-walled beam undergoes torsional deformation only, the displacement functions $u_p(x, t)$, $v_p(x, t)$ and $w_p(x, t)$ represent the torsional deformation at an arbitrary point $p(y, z)$ are given by:

$$u_p(x, t) = \omega(s)\phi'(x, t), \quad v_p(x, t) = -z(s)\phi(x, t), \quad \text{and} \quad w_p(x, t) = y(s)\phi(x, t) \quad (1)$$

where $\phi(x, t)$ is the torsional displacement, $x(s)$ and $y(s)$ are the coordinates of arbitrary point $p(y, z)$ along the principal axes Y and Z , respectively, $\omega(s) = \int_s h(s)ds$ is the warping function of the cross-section defined by Vlasov (1960), in which $h(s) = x(s)(dy/ds) - y(s)(dx/ds)$ is the perpendicular distance from the shear center S_c to the tangent to the mid-surface at point $p(y, z)$. The present formulation is focused on linear response of the thin-walled beams under small displacements, the non-zero normal strain is given as:

$$\varepsilon_{xx} = \frac{\partial u_p}{\partial x} = \omega(s)\phi''(x, t) \quad (2)$$

Hamilton Variational Principle

To formulate the torsional dynamic field equation, the form of Hamilton's principle is given as:

$$\int_{t_1}^{t_2} \delta(T - \Pi) dt = \int_{t_1}^{t_2} \delta T dt - \int_{t_1}^{t_2} \delta(U + V) dt = 0, \quad \text{for } \delta\phi(x, t) = 0 \text{ at } t = t_1 = t_2 \quad (3)$$

where, T represents the total kinetic energy of the thin-walled beam, while Π denotes the total potential energy, which is the combination of the elastic strain energy U stored in the deformed beam and the potential energy V associated with applied harmonic torsional and warping moments. The symbol δ indicates the variation operator, and the integration is carried out over the time interval from t_1 to t_2 . The expression for the first variation of the total kinetic energy δT is presented as follows:

$$\delta T = \int_0^L \int_A \rho [\dot{u}_p \delta u_p + \dot{v}_p \delta v_p + \dot{w}_p \delta w_p] dA dx = \int_0^L \rho [C_w \dot{\phi}' \delta \phi' + AI_o^2 \dot{\phi} \delta \dot{\phi}] dx \quad (4)$$

where C_w is the warping constant defined by $C_w = \int_A (\omega(s))^2 dA$, the polar radius of gyration about the shear center is $I_o^2 = (I_y + I_z)/A$, in which A is the area of the cross-section, and ρ is the material density, The first variation of the internal strain energy δU is given by:

$$\delta U = \int_0^L \int_A E \varepsilon_{xx} \delta \varepsilon_{xx} dAdz + \int_0^L GJ \phi' \delta \phi' dz = \int_0^L [EC_w \phi'' \delta \phi'' + GJ \phi' \delta \phi'] dx \quad (5)$$

in which the second term in equation (5) is the contribution of Saint Venant shear strain, E is the modulus of elasticity, G is the shear modulus, and J is the St. Venant torsional constant. All primes denote derivatives with respect to space coordinate x whereas dots denote the derivatives with respect to time t .

The variation of potential energy δV due to the applied harmonic torsional moment $m_x(x, t)$ along beam axis and concentrated torsional moments $M_x(x, t)$ and concentrated warping moments $M_w(x, t)$ applied at beam ends (i.e., $x = 0, L$) is given as:

$$\delta V = \int_0^L m_x(x, t) \delta \phi(x, t) dx + [M_x(x, t) \delta \phi(x, t) + M_w(x, t) \delta \phi'(x, t)]_0^L \quad (6)$$

In equation (6), $m_x(x, t)$ is the harmonic distributed torsional moment, $M_x(x, t)$ are the harmonic concentrated torsional moments and $M_w(x, t)$ are the harmonic concentrated warping moments applied at beam ends (i.e., $x = 0, L$). All applied torsional moments are assumed to have the same sign convention as those of the end torsional deformations (Fig. 1).

From equations (4-6) and by substituting into equation (3), performing integration by parts with respect to time; evoking the stationary condition of the Hamilton's functional; noting that all the variations of the coefficients at the time limits t_1 and t_2 are zero, i.e., $\delta \phi(z, t)|_{t_1}^{t_2} = 0$, one obtains the torsional dynamic field equation as:

$$\rho A I_o^2 \ddot{\phi}(x, t) - \rho C_w \ddot{\phi}''(x, t) + EC_w \phi''''(x, t) - GJ \phi''(x, t) = m_x(x, t) \quad (7)$$

The related boundary conditions are obtained as:

$$[EC_w \phi'''' - GJ \phi'' - M_x(x, t)]_0^L \delta \phi(x, t)|_0^L = 0 \quad (8)$$

$$[EC_w \phi'' - M_w(x, t)]_0^L \delta \phi'(x, t)|_0^L = 0 \quad (9)$$

Equation (7) presents the governing field equation for the torsional vibration of open thin-walled Vlasov doubly symmetric beam under distributed harmonic torsional and warping moments. It shows that the warping not only influences the deformation of thin-walled beam but also impacts its dynamic behavior due to the associated mass distribution, in which the warping inertia is accounted for in the governing field equation for a thin-walled beam under distributed harmonic torsional loading.

Expressions for Applied Moments and Displacements

The thin-walled beam is assumed to be subjected to distributed harmonic twisting moment $m_x(x, t)$ and concentrated twisting moment $M_x(x, t)$ and warping moment $M_w(x, t)$ applied at beam ends as:

$$m_x(x, t), M_x(x, t), M_w(x, t) = [\bar{m}_x(x), \bar{M}_x(x), \bar{M}_w(x)] e^{i\Omega t} \quad (10)$$

Under the given harmonic torsional moments, the torsional rotation function $\phi(z, t)$ corresponding to the steady-state component of the dynamic response is assumed to take the form:

$$\phi(x, t) = \bar{\phi}(x) e^{i\Omega t} \quad (11)$$

in which $i = \sqrt{-1}$ is the imaginary constant, $\bar{\phi}(x)$ is the torsional space function. Since the present formulation is designed to capture only the steady-state dynamic response of the system, the torsional rotation function proposed in equation (11) excludes the transient component of the dynamic response. From equations (10-11) and by substituting into equation (7), one obtains:

$$EC_w \mathcal{D}^4 \bar{\phi}(x) - \rho A \Omega^2 I_o^2 \bar{\phi}(x) + (\rho \Omega^2 C_w - GJ) \mathcal{D}^2 \bar{\phi}(x) = \bar{m}_x(x) \quad (12)$$

and the boundary conditions are obtained as:

$$[EC_w \bar{\phi}'''' - GJ \bar{\phi}'' - \bar{M}_x(x)]_0^L \delta \bar{\phi}(x)|_0^L = 0 \quad (13)$$

$$[EC_w \bar{\phi}'' - \bar{M}_w(x)]_0^L \delta \bar{\phi}'(x)|_0^L = 0 \quad (14)$$

where \mathcal{D} is the differential operator, i.e., $\mathcal{D}^2 \equiv d^2/dz^2$, and $\mathcal{D}^4 = d^4/dz^4$.

Exact Homogeneous Solution for Torsional Equation

The homogeneous solution of the field equation (12) is obtained by setting the loading term in the field equation to zero, i.e., $\bar{m}_x(x) = 0$. The solution of the torsional rotation space function $\bar{\phi}(x)$ is then assumed to take the following form:

$$\bar{\phi}(x) = A_i e^{m_i x}, \text{ for } i = 1,2,3,4 \quad (15)$$

From of space torsional function postulated in equation (15), by substituting into the torsional equation (12), one obtains the quartic algebraic equation as:

$$EC_w m_i^4 + (\rho\Omega^2 C_w - GJ)m_i^2 - \rho A\Omega^2 I_o^2 = 0 \quad (16)$$

The resulting equation (16) is solved for constants yielding the roots as:

$$m_{1,2} = \pm \left[\frac{-(\rho\Omega^2 C_w - GJ) + \sqrt{(\rho\Omega^2 C_w - GJ)^2 + 4EC_w \rho A\Omega^2 I_o^2}}{2EC_w} \right]^{1/2} = \pm \beta, \text{ and}$$

$$m_{3,4} = \pm i \left[\frac{(\rho\Omega^2 C_w - GJ) + \sqrt{(\rho\Omega^2 C_w - GJ)^2 + 4EC_w \rho A\Omega^2 I_o^2}}{2EC_w} \right]^{1/2} = \pm i\alpha$$

It is noted that, the four roots (m_i for $i = 1,2,3,4$) are distinct and the homogeneous solution for torsional rotation function $\bar{\phi}(x)$ is obtained as:

$$\bar{\phi}(x) = c_1 \cosh(\beta x) + c_2 \sinh(\beta x) + c_3 \cos(\alpha x) + c_4 \sin(\alpha x) \quad (17)$$

where c_i for $i = 1,2,3,4$ are unknown integration constants which can be obtained from the problem boundary conditions. The exact homogeneous solution related to steady state torsional response presented in equation (17) can be written in matrix form as:

$$\bar{\phi}(x) = \langle \chi(x) \rangle_{1 \times 4} \{C\}_{4 \times 1} \quad (18)$$

where $\langle \chi(x) \rangle_{1 \times 4} = \langle \cosh(\beta x) \sinh(\beta x) \cos(\alpha x) \sin(\alpha x) \rangle_{1 \times 4}$, and $\langle C \rangle_{1 \times 4} = \langle c_1 \ c_2 \ c_3 \ c_4 \rangle_{1 \times 4}$.

Finite Element Formulation

The developed finite beam element is designed to analyze the steady state torsional response of open thin-walled doubly symmetric beams subjected to various harmonic torsional and warping moments. The two-noded finite beam element, with four degrees of freedom per element (Fig. 2), is formulated using exact shape functions that precisely satisfy the homogeneous solution of the torsional field equation. These functions are utilized to derive the exact stiffness and mass matrices, as well as the load potential energy vector for the beam element.

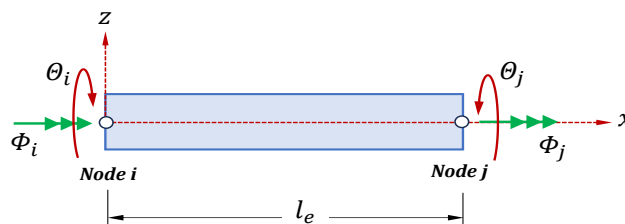


Figure 2: Two-noded thin-walled beam element for torsional-warping response.

Formulating of Exact Shape Functions

To relate the torsional displacement $\bar{\phi}(x)$ to nodal torsional displacements, the vector of unknown integration constants $\langle C \rangle_{1 \times 4} = \langle c_1 \ c_2 \ c_3 \ c_4 \rangle_{1 \times 4}$ is represented in terms of torsional rotation and rate of torsional displacement $\langle \Psi_N \rangle_{1 \times 4} = \langle \theta_1 \ \phi_1 \ \theta_2 \ \phi_2 \rangle_{1 \times 4}$ by applying the following conditions $\theta_1 = \bar{\phi}(0)$, $\phi_1 = \bar{\phi}'(0)$, $\theta_2 = \bar{\phi}(l_e)$, and $\phi_2 = \bar{\phi}'(l_e)$. This leads to:

$$\{\Psi_e\}_{4 \times 1} = \begin{Bmatrix} \theta_1 \\ \phi_1 \\ \theta_2 \\ \phi_2 \end{Bmatrix}_{4 \times 1} = \begin{Bmatrix} \bar{\phi}(0) \\ \bar{\phi}'(0) \\ \bar{\phi}(l_e) \\ \bar{\phi}'(l_e) \end{Bmatrix}_{4 \times 1} = \begin{bmatrix} \langle \chi(0) \rangle_{1 \times 4} \\ \langle \chi'(0) \rangle_{1 \times 4} \\ \langle \chi(l_e) \rangle_{1 \times 4} \\ \langle \chi'(l_e) \rangle_{1 \times 4} \end{bmatrix}_{4 \times 4} \{C\}_{4 \times 1} = [F]_{4 \times 4} \{C\}_{4 \times 1} \quad (19)$$

$$\text{in which } [\mathcal{F}]_{4 \times 4} = \begin{bmatrix} 1 & 0 & 1 & 0 \\ 0 & \beta & 0 & \alpha \\ \cosh(\beta l_e) & \sinh(\beta l_e) & \cos(\alpha l_e) & \sin(\alpha l_e) \\ \beta \sinh(\beta l_e) & \beta \cosh(\beta l_e) & -\alpha \sin(\alpha l_e) & \alpha \cos(\alpha l_e) \end{bmatrix}_{4 \times 4}$$

From equation (19), by substituting into equation (18), one obtains:

$$\bar{\phi}(x) = \langle \chi(x) \rangle_{1 \times 4} [\mathcal{F}]_{4 \times 4}^{-1} \langle \Psi_e \rangle_{4 \times 1} = \langle H(x) \rangle_{1 \times 4} \langle \Psi_e \rangle_{4 \times 1} \quad (20)$$

where $\langle H(x) \rangle_{1 \times 4} = \langle \chi(x) \rangle_{1 \times 4} [\mathcal{F}]_{4 \times 4}^{-1}$ is the exact shape function matrix for the torsional-warping response of open thin-walled doubly symmetric beams, it is observed that the shape functions presented in equation (20) precisely satisfy the homogeneous solution of the torsional field equation.

Energy Expressions in Terms of Nodal Torsional Displacements

The expressions for the variation of kinetic energy, strain energy, and the potential by applied harmonic torsional and warping moments, along with the axial static force, are derived in terms of the nodal degrees of freedom. This is achieved by substituting equation (20) into equations (4-6), resulting in the following:

$$\delta T = -\langle \delta \Psi_e \rangle_{1 \times 4} \left(\Omega^2 \int_0^{l_e} (\rho C_w + \rho A I_o^2) \{H(x)\}_{4 \times 1} \langle H(x) \rangle_{1 \times 4} dx \right) \langle \Psi_e \rangle_{4 \times 1} e^{i\Omega t} dx \quad (21)$$

$$\delta U = \langle \delta \Psi_e \rangle_{1 \times 4} \left(\int_0^{l_e} [EC_w \{H''(x)\}_{4 \times 1} \langle H''(x) \rangle_{1 \times 4} + GJ \{H'(x)\}_{4 \times 1} \langle H'(x) \rangle_{1 \times 4}] \langle \Psi_e \rangle_{4 \times 1} e^{i\Omega t} dx \right) \quad (22)$$

$$\delta V = \langle \delta \Psi_e \rangle_{1 \times 4} \left(\int_0^{l_e} \bar{m}_x(x) \{H(x)\}_{4 \times 1} dx + [\bar{M}_x(x) \{H(x)\}_{4 \times 1} + \bar{M}_w(x) \{H'(x)\}_{4 \times 1}]_0^{l_e} \right) e^{i\Omega t} \quad (23)$$

From equations (21-23), by substituting into Hamilton's variational principle (eqn. 3), one obtains:

$$([K_e]_{4 \times 4} - \Omega^2 [M_e]_{4 \times 4}) \langle \Psi_e \rangle_{4 \times 1} = \langle F_e \rangle_{4 \times 1} \quad (24)$$

in which, the stiffness matrix for beam element $[K_e]_{4 \times 4}$ is given by:

$$[K_e]_{4 \times 4} = \int_0^{l_e} [GJ \{H'(x)\}_{4 \times 1} \langle H'(x) \rangle_{1 \times 4} + EC_w \{H''(x)\}_{4 \times 1} \langle H''(x) \rangle_{1 \times 4}] dx$$

The mass matrix for beam element $[M_e]_{4 \times 4}$ is given by:

$$[M_e]_{4 \times 4} = \int_0^{l_e} (\rho A I_o^2 - \rho C_w) \{H(x)\}_{4 \times 1} \langle H(x) \rangle_{1 \times 4} dx$$

The element load vector $\langle F_e \rangle_{4 \times 1}$ is given by:

$$\langle F_e \rangle_{4 \times 1} = \int_0^{l_e} \bar{m}_x(x) \{H(x)\}_{4 \times 1} dx + [\bar{M}_x(x) \{H(x)\}_{4 \times 1} + \bar{M}_w(x) \{H'(x)\}_{4 \times 1}]_0^{l_e}$$

The elastic stiffness and mass matrices, along with the load vector for a one-dimensional, two-noded thin-walled beam element with two degrees of freedom per node, are computed for torsional vibration analysis using the exact shape functions derived in this formulation.

Galerkin Finite Element Formulation

The trial solution is assumed to take the form:

$$\bar{\phi}(x) = \sum_{i=1}^4 N_i(x) u_i \quad (25)$$

where $N_i(x)$ are the shape functions for beam element, and $u_1 = \phi_1$, $u_2 = \phi_1'$, $u_3 = \phi_2$, and $u_4 = \phi_2'$.

The weak form is obtained by multiplying the governing equation (13) by the weight function $N_i(x)$ as:

$$\int_0^{l_e} N_i(x) [EC_w \mathcal{D}^4 \bar{\phi}(x) - \rho A \Omega^2 I_o^2 \bar{\phi}(x) + (\rho \Omega^2 C_w - GJ) \mathcal{D}^2 \bar{\phi}(x) - \bar{m}_x(x)] dx = 0$$

By integrating the previous equation over the beam element length l_e to reduce the order of derivatives, and then applying the related boundary conditions presented in (14) and (15), leads to the following system:

$$([\bar{K}_e]_{4 \times 4} - \Omega^2 [\bar{M}_e]_{4 \times 4}) \{u_e\}_{4 \times 1} = \langle \bar{F}_e \rangle_{4 \times 1} \quad (26)$$

where $[\bar{K}_e]_{4 \times 4}$ is the stiffness matrix for beam element, $[\bar{M}_e]_{4 \times 4}$ is the element mass matrix, $\langle \bar{F}_e \rangle_{4 \times 1}$ is the vector of applied forces, and $\{u_e\}_{4 \times 1}$ is the vector contains the nodal displacements and rotations obtained from Galerkin finite element formulation.

In which, the element stiffness matrix $[\bar{K}_e]_{4 \times 4}$ is obtained by:

$$[\bar{K}_e]_{4 \times 4} = \sum_{j=1}^4 \int_0^{l_e} \left[EC_w \frac{d^2 N_i(x)}{dx^2} \frac{d^2 N_j(x)}{dx^2} + GJ \frac{dN_i(x)}{dx} \frac{dN_j(x)}{dx} \right] dx$$

The element mass matrix $[\overline{M}_e]_{4 \times 4}$ is given as:

$$[\overline{M}_e]_{4 \times 4} = \sum_{j=1}^4 \int_0^{l_e} \left[\rho A I_0^2 N_i(x) N_j(x) + \rho C_w \frac{dN_i(x)}{dx} \frac{dN_j(x)}{dx} \right] dx$$

while the element force vector $\{\overline{F}_e\}_{4 \times 1}$ is obtained as:

$$\{\overline{F}_e\}_{4 \times 1} = \int_0^{l_e} \overline{m}_x(x) N_i(x) dx - [\overline{M}_x(x) N_i(x)]_0^{l_e} + \left[\overline{M}_w(x) \frac{dN_i(x)}{dx} \right]_0^{l_e}$$

For C^1 problem, the approximate shape functions $N_1(x), N_2(x), N_3(x)$ and $N_4(x)$ in element local coordinates are given as:

$$\begin{aligned} N_1(x) &= \frac{1}{l_e^3} (2x^3 - 3x^2 l_e + l_e^3), & N_2(x) &= \frac{1}{l_e^3} (x^3 l_e - 2x^2 l_e^2 + x l_e^3) \\ N_3(x) &= \frac{1}{l_e^3} (-2x^3 + 3x^2 l_e), & \text{and} & \\ N_4(x) &= \frac{1}{l_e^3} (x^3 l_e - x^2 l_e^2) \end{aligned} \quad (27)$$

These shape functions ensure both displacement and rotation continuity at the element nodes. Substituting equation (27) into stiffness, mass matrices and force vector to obtain:

$$[\overline{K}_e] = EC_w \begin{bmatrix} \frac{12}{l_e^3} & \frac{6}{l_e^2} & -\frac{12}{l_e^2} & \frac{6}{l_e^2} \\ \frac{6}{l_e^2} & \frac{4}{l_e} & -\frac{6}{l_e} & \frac{2}{l_e} \\ -\frac{12}{l_e^2} & -\frac{6}{l_e} & \frac{12}{l_e^2} & -\frac{6}{l_e} \\ \frac{6}{l_e^2} & \frac{2}{l_e} & -\frac{6}{l_e} & \frac{4}{l_e} \end{bmatrix} + GJ \begin{bmatrix} -\frac{6}{5l_e} & -\frac{1}{10} & \frac{6}{5l_e} & -\frac{1}{10} \\ \frac{-1}{10} & -\frac{2l_e}{15} & \frac{1}{10} & \frac{l_e}{30} \\ \frac{6}{5l_e} & \frac{1}{10} & -\frac{6}{5l_e} & \frac{1}{10} \\ -\frac{1}{10} & \frac{l_e}{30} & \frac{1}{10} & -\frac{2l_e}{15} \end{bmatrix},$$

$$[\overline{M}_e] = (\rho A \Omega^2 I_0^2) \begin{bmatrix} -\frac{13l_e}{35} & -\frac{11l_e^2}{210} & -\frac{9l_e}{70} & \frac{13l_e^2}{420} \\ \frac{-11l_e^2}{210} & -\frac{l_e^3}{105} & -\frac{13l_e^2}{420} & \frac{l_e^3}{140} \\ \frac{-9l_e}{70} & -\frac{13l_e^2}{420} & -\frac{13l_e}{420} & \frac{11l_e^2}{210} \\ \frac{13l_e^2}{420} & \frac{l_e^3}{140} & \frac{11l_e^2}{210} & -\frac{l_e^3}{105} \end{bmatrix} + (\rho \Omega^2 C_w) \begin{bmatrix} -\frac{6}{5l_e} & -\frac{1}{10} & \frac{6}{5l_e} & -\frac{1}{10} \\ \frac{-1}{10} & -\frac{2l_e}{15} & \frac{1}{10} & \frac{l_e}{30} \\ \frac{6}{5l_e} & \frac{1}{10} & -\frac{6}{5l_e} & \frac{1}{10} \\ -\frac{1}{10} & \frac{l_e}{30} & \frac{1}{10} & -\frac{2l_e}{15} \end{bmatrix}, \text{ and}$$

$$\text{the vector of applied forces is given as: } \{\overline{F}_e\} = \begin{Bmatrix} \frac{\overline{m}(x).l_e}{2} + \overline{M}_x(0) \\ \frac{\overline{m}(x).l_e^2}{12} - \overline{M}_w(0) \\ \frac{\overline{m}(x).l_e}{2} + \overline{M}_x(l_e) \\ -\frac{\overline{m}(x).l_e^2}{12} + \overline{M}_w(l_e) \end{Bmatrix}.$$

Numerical Examples and Validation

This section presents two examples for thin-walled beams with doubly symmetric open cross-sections, subjected to various harmonic torsional and warping moments under different boundary conditions, to demonstrate the validity, accuracy, and applicability of the developed exact finite two-noded thin-walled beam element. The beam element is utilized to: (a) compute the steady-state torsional dynamic response of the thin-walled beam under specified torsional excitations, (b) capture the quasi-static torsional response of the thin-walled beam under torsional excitation having very small exciting frequency, and (c) predict the natural torsional frequencies of the thin-walled beam. The formulation is based on shape functions that exactly satisfy the exact homogeneous solution of the torsional field equation. This approach eliminates mesh discretization errors commonly encountered in conventional interpolation schemes used in finite element solutions, allowing convergence with a minimal number of degrees of freedom. The torsional results obtained from the present finite beam element (with two degrees of freedom per node) are compared to exact solutions and finite element results available in the literature.

Example (1): Static and Dynamic Responses - Validation

In this example, a cantilever thin-walled I-beam with span of 2.40m subjected to three types of harmonic loading: (i) uniformly distributed twisting moment $m_x(x, t) = 2.40e^{i\Omega t} kN.m/m$ along the beam axis, (ii) concentrated twisting moment $M_x(L, t) = 1.80e^{i\Omega t} kN.m$, and (iii) concentrated warping moment $M_w(L, t) = 2.0e^{i\Omega t} kN.m$ applied at the beam free end ($x = L$), as illustrated in Figure (3). The geometric and material properties of the beam cross-section are provided in Table (1). To verify the accuracy of the exact closed-form solution and the

finite beam element model developed in this study, the following tasks are required: (a) performing a quasi-static torsional analysis using a very low excitation frequency, i.e., $\Omega \approx 0.01\omega_{t1}$, and (b) investigating the steady-state dynamic torsional response at exciting frequency of $\Omega = 1.64\omega_{t1}$, where ω_{t1} is the first natural torsional frequency of the cantilever beam obtained as $f_{1t} = 35.26\text{Hz}$.

Table 1: Geometric and properties of doubly symmetric thin-walled I-beam.

Parameter	Value	Parameter	Value
E	$200.0 \times 10^9 \text{ N/m}^2$	A	$7420 \times 10^{-6} \text{ m}^2$
G	$77.0 \times 10^9 \text{ N/m}^2$	ρ	8000 kg/m^3
I_{yy}	$87.10 \times 10^{-6} \text{ m}^4$	I_{zz}	$18.82 \times 10^{-6} \text{ m}^4$
J	$373.7 \times 10^{-9} \text{ m}^4$	C_w	$268.0 \times 10^{-9} \text{ m}^6$

Figure 3: A cantilever thin-walled I-beam under various twisting and warping moments.

The numerical results obtained from the exact closed-form solution and finite element formulation developed in this study based on Vlasov beam theory are compared with those obtained from the exact solutions presented in the literature and Abaqus finite beam element. In the Abaqus finite element model, the thin-walled beam with two nodes is represented using 80 B31OS elements (i.e., 567 dof) along the beam axis to achieve high accuracy. In contrast, the present finite element model uses a single two-noded beam element (i.e., 4 dof) to match the exact solution. Although the present finite beam element results are obtained using a single beam element, five beam elements with 12 degrees of freedom are used for a more detailed comparison with the Abaqus solution, in order to demonstrate better match with the nodal results.

Quasi-Static Analysis for Torsional Response

To achieve the quasi-static torsional response of a cantilever thin-walled beam under various harmonic twisting and warping moments, the excitation frequency Ω is set significantly lower than the first natural torsional frequency, specifically $\Omega \approx 0.01\omega_1 = 2.215\text{rad/sec}$. Table (2) presents a comparative analysis of the quasi-static results for torsional rotation angles $\bar{\phi}(L)$ and warping functions $\bar{\phi}'(L)$, demonstrating the accuracy of the finite element solution (FES) in modeling the torsional behavior of thin-walled cantilever I-beams. The results exhibit a high degree of agreement across models, with the static solutions aligning closely with those reported by Hjaji et al. [12] and Seaburg et al. [2]. Notably, the results from the present FE solution and those from Hjaji et al. [12] and Abaqus mode (AFS) are nearly identical, indicating the reliability of these computational

Table 2: Static results for torsional rotation angle $\bar{\phi}(L)$ and warping function $\bar{\phi}'(L)$ for thin-walled cantilever I-beam under various twisting and warping moments.

Type of load	Function ($\times 10^{-3}$)	Hjaji et al. [12]	Seaburg et al. [2]	Abaqus FES	Present FES
Distributed twisting moment $m_x(x, t)$	$\bar{\phi}(L)$	-86.668	-86.129	-86.994	-86.129
	$\bar{\phi}'(L)$	-40.420	-40.275	-40.566	-40.276
End twisting moment $M_x(L, t)$	$\bar{\phi}(L)$	-69.911	-69.679	-69.935	-69.679
	$\bar{\phi}'(L)$	-41.536	-41.619	-41.567	-41.619
End warping moment $M_w(L, t)$	$\bar{\phi}(L)$	-46.151	-	-46.185	-46.243
	$\bar{\phi}'(L)$	-48.080	-	-48.112	-47.989
Various moments $m_x(x, t)$, $M_x(L, t)$, and $M_w(L, t)$	$\bar{\phi}(L)$	-202.73	-	-203.10	-202.05
	$\bar{\phi}'(L)$	-129.83	-	-130.20	-129.88

approaches. Minor deviations between the present FE solution (FES) and other models likely arise from shear deformation effects, which are considered in Hjaji et al. [12] and Abaqus (AFS) but not in Seaburg et al. [2] and FES. Excellent static results for the nodal torsional angle θ_n and warping deformation function Φ_n (for $n = 1,2,3,4,5$) are achieved using the proposed finite element formulation with a single beam element and 4 degrees

of freedom. However, for a broader comparison with the Abaqus finite element solution, which employs 80 B31OS elements and 567 degrees of freedom, five finite elements are utilized for the sake of comparison. Figure (4) illustrates the nodal torsional rotation θ_n and warping deformation function Φ_n for the cantilever I-beam subjected to various harmonic twisting and warping moments. The results, including the exact solutions by Hjaji et al. [12], Seaburg et al. [2], Abaqus finite element solutions, and the proposed finite element solution, are overlaid for comparison. It is evident that the proposed finite element solution exhibits excellent agreement with

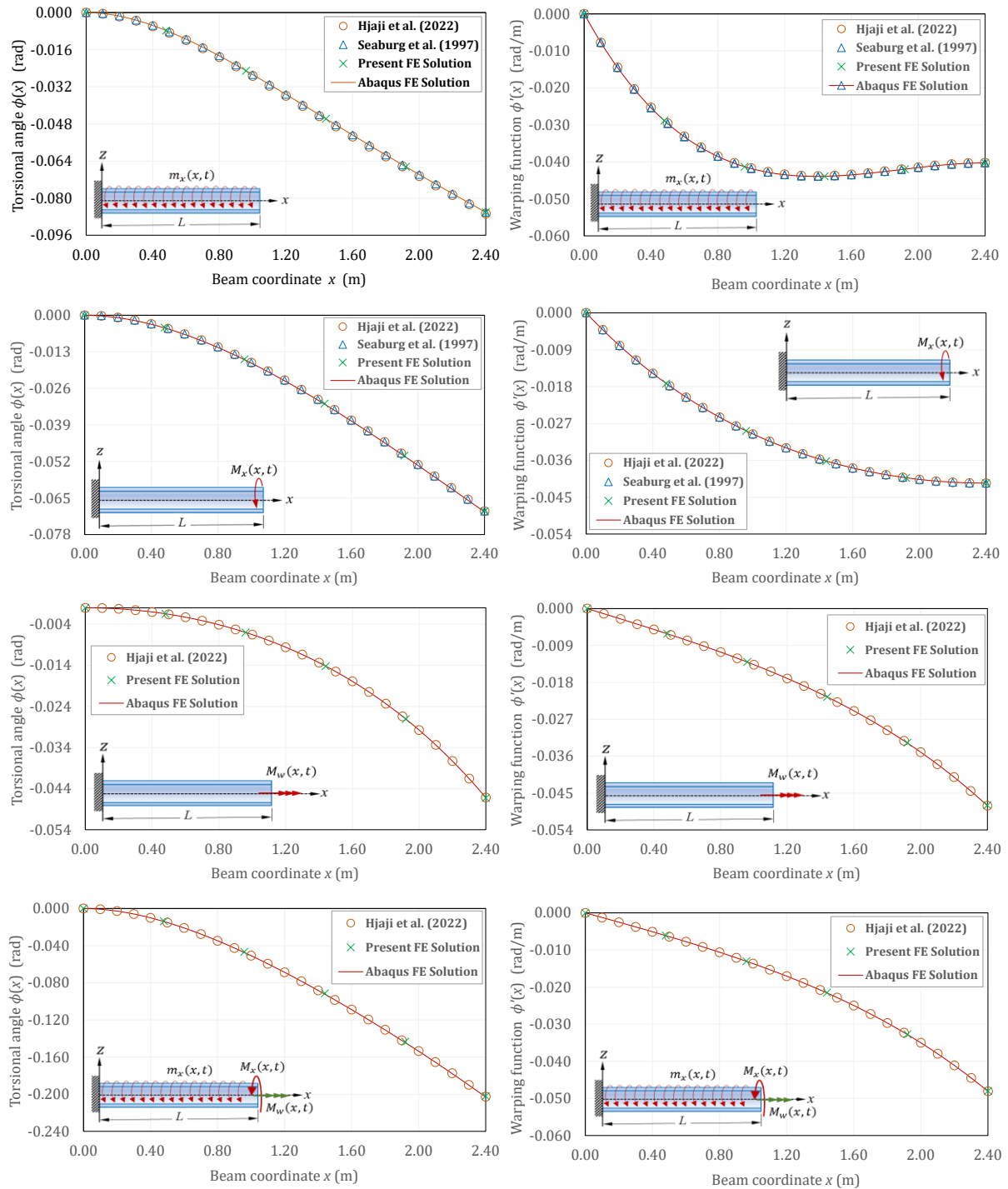


Figure 4: Static torsional response for cantilever thin-walled beam under various torsional and warping moments.

the other solutions. This alignment naturally arises because the present finite element solution employs shape functions that precisely satisfy the homogeneous form of the torsional equation are used. As a result, this approach effectively eliminates the discretization errors commonly introduced in traditional finite element formulations. Overall, the present FE solution effectively captures the static torsional behavior of thin-walled members.

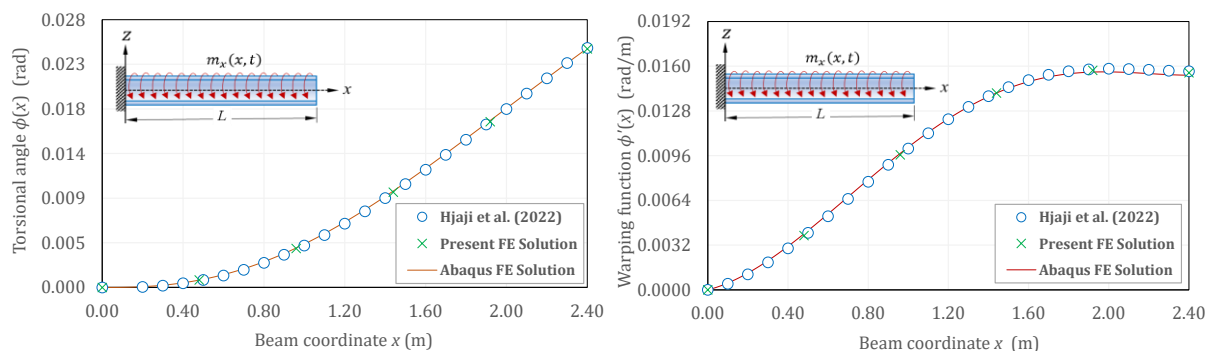
Dynamic response analysis

The dynamic response analysis focuses on evaluating the nodal torsional rotation angle and warping deformation function at the free end of a cantilever I-beam subjected to various harmonic torsional and warping moment loads, with exciting frequency $\Omega = 2.232\omega_{t1} = 494.4 \text{ rad/sec}$, is summarized in Table (3). The steady-state dynamic results obtained from the present finite element solution (FES), using a single beam element with four degrees of freedom per element, are compared with the exact solution provided by Hjaji et al. [12], and Abaqus finite element model (AFE) employing 80 B31OS elements with 567 degrees of freedom for enhanced accuracy. It is noted that, the dynamic response results highlight the close agreement between these three solutions, exhibiting the reliability of the present finite element solution (FES). Notably, the present FE solution demonstrates consistent performance, with deviations observed to be within acceptable limits when compared to established references.

Table 3: Dynamic results of torsional rotation angle $\bar{\phi}(L)$ and warping function $\bar{\phi}'(L)$ for thin-walled cantilever I-beam under various twisting and warping moments.

Type of load	Function ($\times 10^{-3}$)	Hjaji et al. [12]	Abaqus AFE	Present FES
Distributed twisting moment $m_x(x, t)$	$\bar{\phi}(L)$	24.688	24.652	24.675
	$\bar{\phi}'(L)$	15.636	15.364	15.508
End twisting moment $M_x(L, t)$	$\bar{\phi}(L)$	-11.266	-11.330	-11.621
	$\bar{\phi}'(L)$	2.8879	2.8403	2.4464
End warping moment $M_w(L, t)$	$\bar{\phi}(L)$	3.2087	3.1559	2.9275
	$\bar{\phi}'(L)$	29.904	29.808	29.169
Various moments $m_x(x, t)$, $M_x(L, t)$, and $M_w(L, t)$	$\bar{\phi}(L)$	16.636	16.478	15.982
	$\bar{\phi}'(L)$	48.430	48.012	47.123

To give comprehensive comparison, the dynamic response results of the nodal torsional rotation θ_n and warping deformation function Φ_n (for $n = 1, 2, 3, 4, 5$) for the given cantilever beam are plotted against the beam axis x as illustrated in Figures (5). The nodal degrees of freedom results based on three solutions: the finite element solution (FES) developed in this study using five beam elements with 12 dof, exact solution (ES) in Hjaji et al. [12], and Abaqus finite element (AFE) using 80 B31OS beam elements, are plotted on the same diagrams for the comparison. It is noted that, the present finite element provides an excellent agreement with those based on Abaqus solution at a fraction of the computational and modelling cost. This outcome is expected, as the present beam element is constructed using shape functions that precisely satisfy the exact solution of the torsional field equation, effectively eliminating discretization errors encountered under other interpolation schemes. This emphasizes the accuracy of the proposed solutions in capturing the steady state dynamic torsional response of thin-walled beams under complex dynamic loading scenarios.



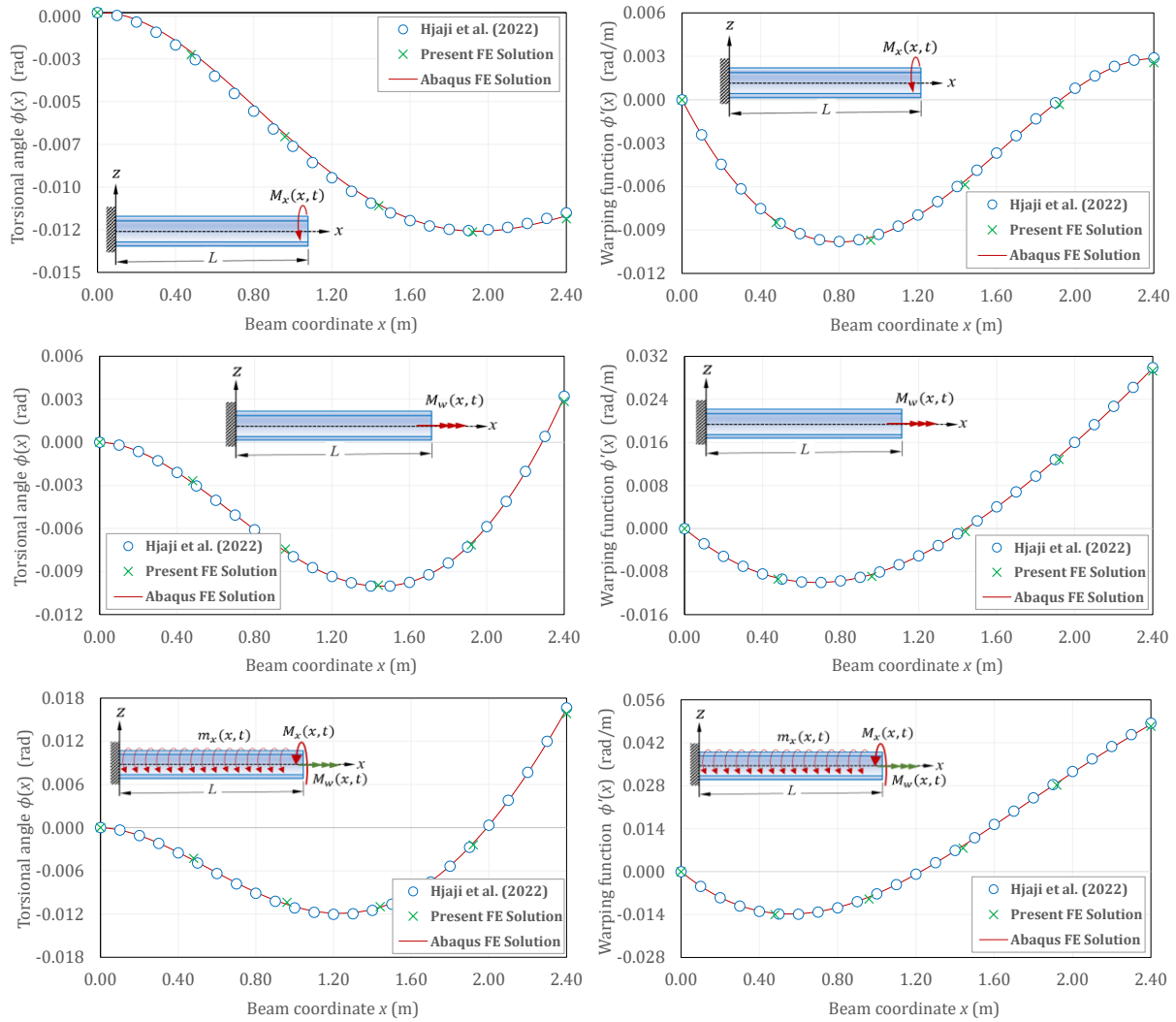


Figure 5: Dynamic torsional response for cantilever thin-walled I-beam under various torsional and warping moments.

Example (2): Torsional natural frequencies

To attain the accuracy of the present finite element formulation to predict the natural torsional frequencies, a 3000mm thin-walled beam subjected to distributed harmonic twisting moment $m_x(x, t) = 1.60e^{i\Omega t} \text{ kNm/m}$ applied along the beam coordinate x is shown in Figure (6). The beam with clamped-free (CF), simply-supported (SS) or fork-fork, clamped-clamped (CC), and clamped-pinned (CS) or clamped-fork boundary conditions are considered in this example. For the case of simply-supported boundary conditions, the fork-type end supports are used, in which the beam is unrestrained along its length while the fork supports prevent the cross-section from torsional rotation and allow free warping deformation. The material and geometrical properties of the steel beam are given in Table (4). For verification purposes, it is required to (a) conduct the steady state dynamic analysis for predicting the first three natural torsional frequencies, (b) compute the quasi-static response analysis by adopting an exciting frequency $\Omega \approx 0.01\omega_{t1}$, and (c) establish the steady state dynamic response for exciting frequency $\Omega = 150\text{rad/sec}$.

Table 4: Geometric and material properties of thin-walled beam.

Parameter	Value	Parameter	Value
E	200GPa	G	78GPa
A	7200mm ²	ρ	7800kg/m ³
I_{yy}	41.24 × 10 ⁶ mm ⁴	J	24.0 × 10 ³ mm ⁴
I_{zz}	8.50 × 10 ⁶ mm ⁴	C_w	87.51 × 10 ⁹ mm ⁶

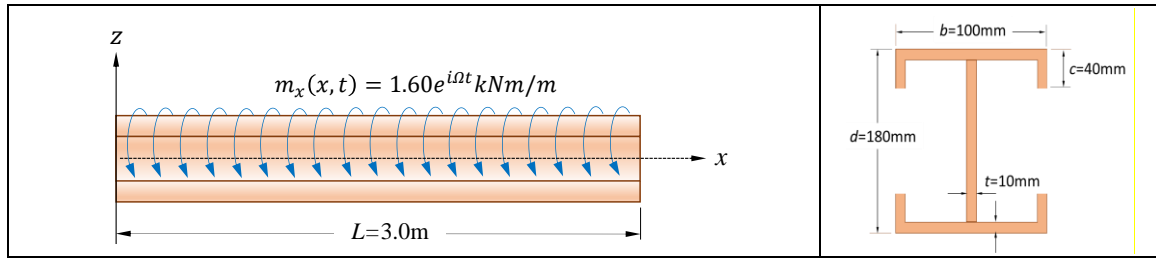


Figure 6: A thin-walled beam under distributed harmonic twisting moment.

The numerical results obtained from the present finite element formulation are compared with corresponding results from other exact solutions available in the literature, as well as with Galerkin and Abaqus finite beam element solutions. In the Abaqus model, the thin-walled beam is discretized using 100 B31OS elements, resulting in a total of 707dof to achieve the desired level of accuracy. In the Galerkin-based finite element approach, the beam is divided into fifty elements, each with four DOF, yielding a total of 102 dof. In contrast, the present finite element formulation uses a single beam element (i.e., 4 dof) to approach the exact results. Even though, the present finite element solution captured the exact nodal results by using one beam element for clamped-free beam and two elements for other beam boundary conditions, this example utilizes six beam elements with 14 dof to exhibit clear observation with Abaqus finite solution based on 100 beam elements (707 dof) and Galerkin finite element model based on 50 beam elements.

Natural Torsional Frequencies

Under the distributed twisting moment $m_x(x, t) = 1.60e^{i\Omega t} kNm/m$, the natural frequencies associated with torsional-warping response are identified through steady-state torsional response analysis. In order to extract the first three natural torsional frequencies for the given beam under clamped-free (CF), simply-supported (SS) or fork-fork, clamped-clamped (CC) and clamped-pinned (CS) or clamped-fork boundary conditions, the exciting frequencies f (in Hz) are varied from near zero to 600Hz, 1800Hz, 2000Hz and 800Hz, respectively. Figures in (4) illustrate the torsional rotation angle $\bar{\phi}(L/2)$ at beam midspan node (i.e., $x = L/2$) as functions of the exciting frequency f . The natural torsional frequencies are determined from the peaks in the torsional rotation-frequency relationship, as these peaks signify resonance. Similarly, peaks observed in the diagrams (Figure 7) serve as indicators of the natural torsional frequencies for the beam.

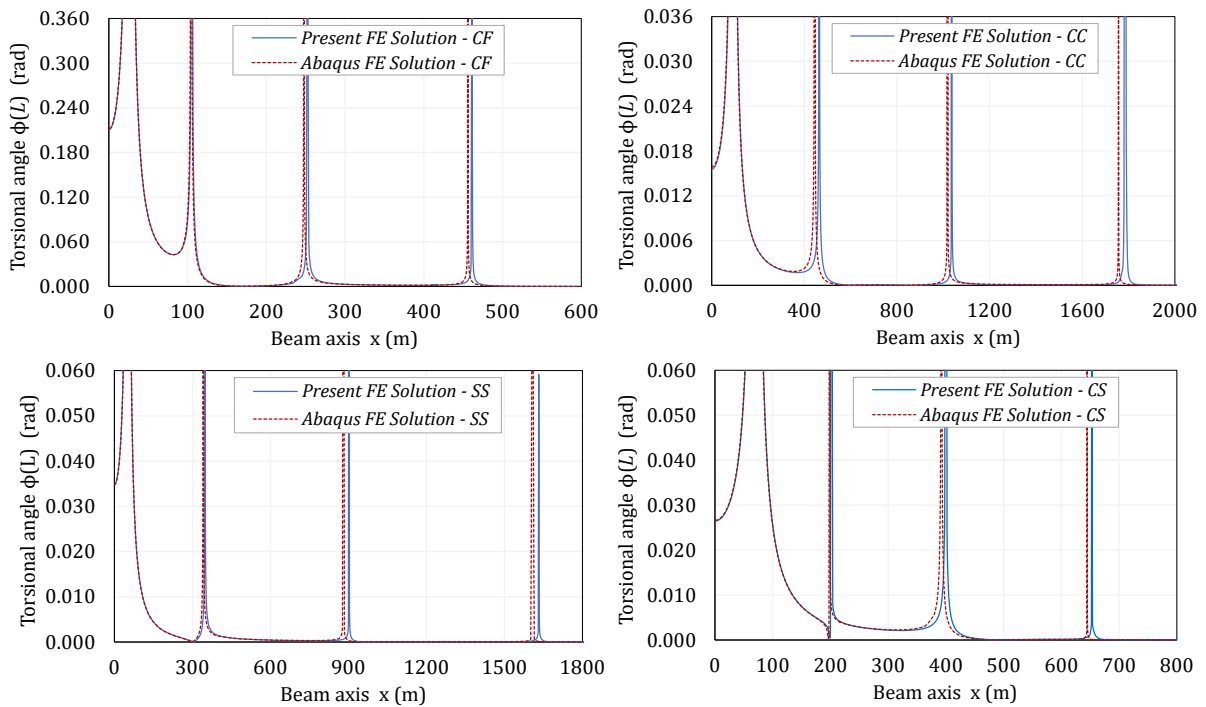


Figure 7: The first four natural torsional frequencies for thin-walled beam under torsional loading with various boundary conditions.

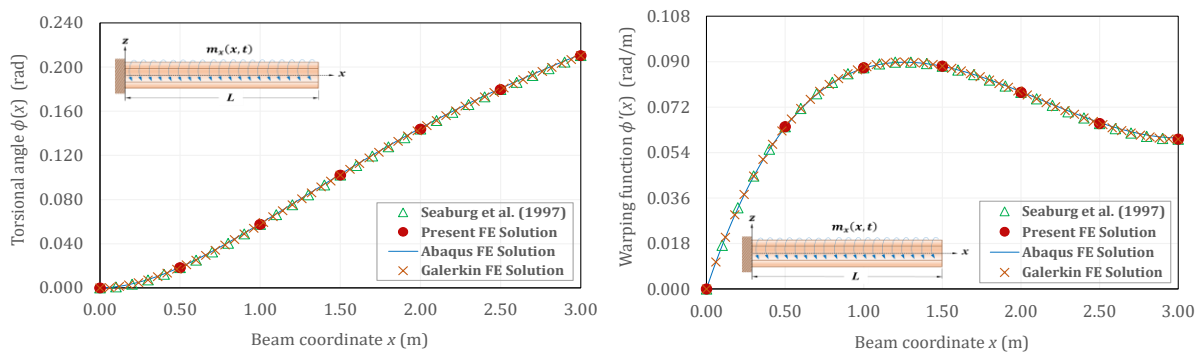
Table (5) is summarized the first three natural torsional frequencies, identified from these resonance peaks. It compares the first three natural torsional frequencies obtained from three different solutions: the present finite element and Galerkin finite element solutions which dis-accounting for shear deformation, while Abaqus finite beam model which considers shear deformation due to bending. The results in Table (5) show that the natural torsional frequencies predicted by the Abaqus finite element model (*AFE*) and Galerkin finite element (*GFE*) differ slightly from those obtained using the present finite element (*PFE*) solution. It is noted that, the frequency results obtained using Galerkin finite element are very close to the corresponding results computed using the present finite element, while Abaqus beam element gives values less close to the present solution. This discrepancy arises naturally because Vlasov beam represents the stiffest beam model (as they neglect shear deformation effects), whereas the Abaqus finite beam analysis provides the most flexible representation due to its consideration of numerous degrees of freedom. The discrepancies arise from the inclusion of shear deformation effects in the Abaqus solution, which are not accounted for in the Vlasov beam theory. Moreover, the variation in results arises because the present finite element utilizes an exact shape function that exactly satisfies the solution of the torsional field equation, whereas the finite element solutions from Abaqus and the Galerkin approach rely on approximate shape functions.

Table 5: The first three natural torsional frequencies for thin-walled beam with various boundary conditions.

Freq No.	Clamped-free			Simply-supported			Clamped-clamped			Clamped-pinned		
	<i>PFE</i>	<i>AFE</i>	<i>GFE</i>	<i>PFE</i>	<i>AFE</i>	<i>GFE</i>	<i>PFE</i>	<i>AFE</i>	<i>GFE</i>	<i>PFE</i>	<i>AFE</i>	<i>GFE</i>
1	26.58	27.04	26.57	52.05	52.75	52.05	93.28	92.01	93.29	69.96	70.61	69.96
2	105.4	104.9	105.2	348.2	341.2	348.2	464.2	444.8	464.2	201.3	198.5	201.7
3	252.2	247.8	251.4	902.3	880.7	922.7	1036	1018	1109	399.4	392.2	403.8

Static Response Analysis

The quasi-static analyzes of the torsional response of thin-walled beam subjected to distributed harmonic twisting moment $m_x(x, t) = 1.60e^{i\Omega t} kNm/m$ are conducted by using very low exciting frequency ($\Omega \approx 0.01\omega_1$) related to the first natural torsional frequency of the given beams. Figures in (8) overlay the nodal torsional rotation angle ϕ_n and warping deformation function ϕ'_n of static torsional responses obtained from the present finite element formulation with the exact solution of Seaburg et al. [2], Abaqus finite element solution using 100 B31OS beam elements (707 dof), and Galerkin finite element solution using 50 beam elements (102 dof). Although the proposed finite element formulation with just two beam elements (6 dof) achieved excellent results, but six beam elements with 14 dof are used for comparison purposes. The results exhibit excellent agreement among all four solutions. It is clearly noted that, the present finite element results using six beam elements (14 dof) closely match those of the Abaqus finite model, which uses 100 beam elements (707 dof) and Galerkin finite element based on 50 elements (102 dof). A gain, these results demonstrate the efficiency and accuracy of the proposed finite element in capturing the static response of the given beam under various boundary conditions.



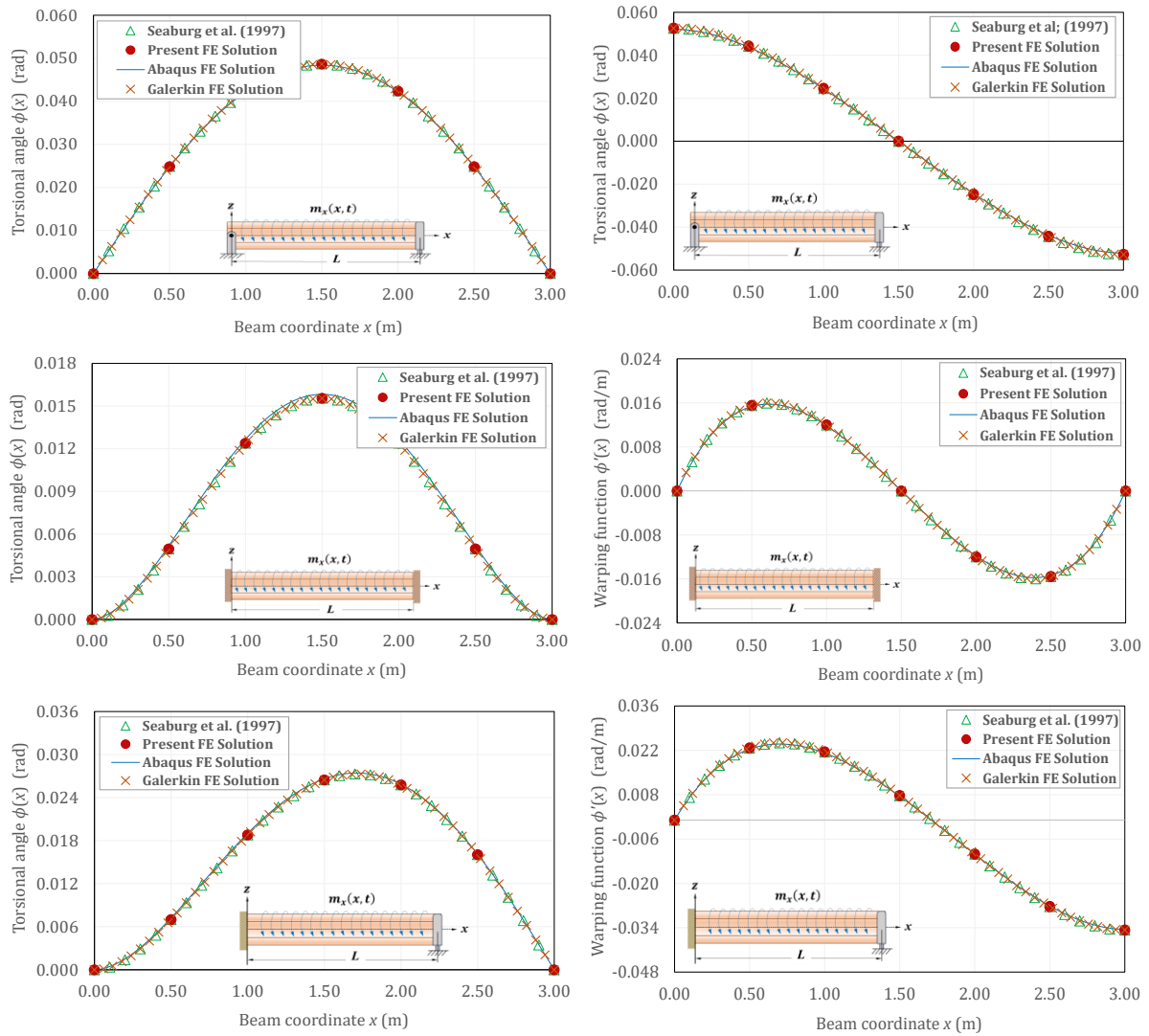
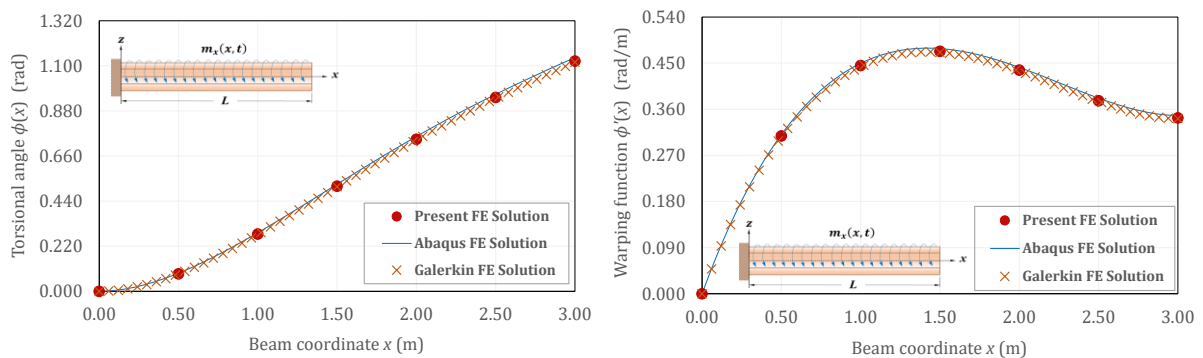


Figure 8: Static torsional responses for thin-walled beam under distributed twisting moment and various boundary conditions.

Steady State Dynamic Response

Figure (9) illustrates the steady-state torsional rotation and warping deformation responses of thin-walled beam subjected to distributed harmonic twisting moment $m_x(x, t) = 1.60e^{i\Omega t} kNm/m$ at exciting frequency $\Omega = 150 rad/sec$. The nodal results for torsional rotation angle θ_n and warping deformation Φ_n ($n = 1, 2, 3, \dots, 7$) derived from the proposed formulations are compared with those obtained using Abaqus finite beam model. The comparison shows that the present closed-form solution and finite element using six beam elements (14 dof) achieves excellent agreement with the Abaqus beam model, which utilizes 100 B310S elements (707 dof) and Galerkin finite element solution based on 50 beam elements.



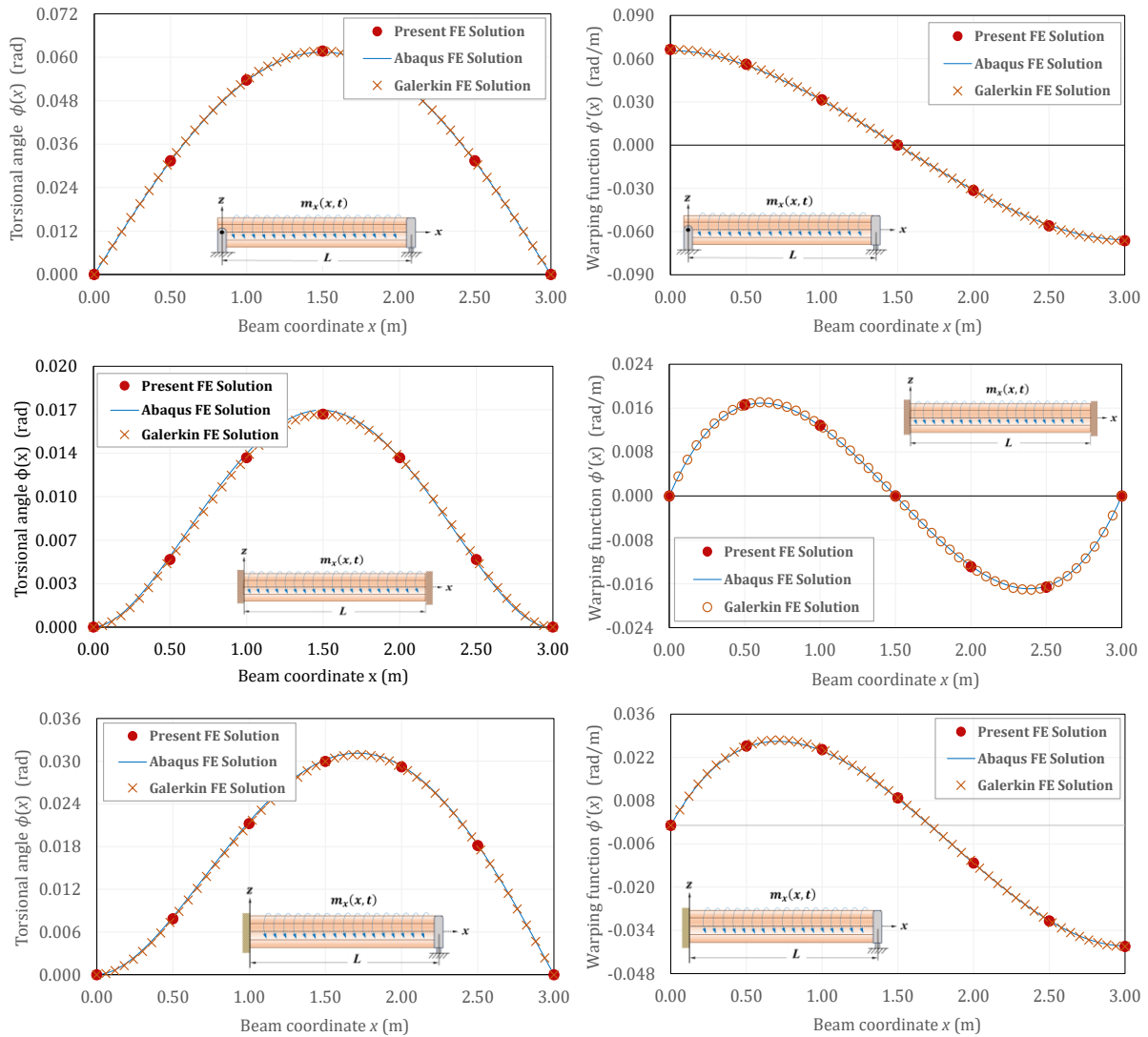


Figure 9: Dynamic torsional responses for thin-walled beams under distributed twisting moment and various boundary conditions.

Example (3) – Validation of Finite beam element Formulation

A thin-walled I-beam of length 6000mm is subjected to various torsional and warping moments; uniformly distributed torsional loading $m_x(x, t) = 1.20e^{i\Omega t} \text{ kNm/m}$ and concentrated twisting moments $M_{x1}(2m, t) = 1.80e^{i\Omega t} \text{ kNm}$ and $M_{x2}(5m, t) = 1.60e^{i\Omega t} \text{ kNm}$ end warping moment $M_w(6m, t) = 1.50e^{i\Omega t} \text{ kNm}^2/\text{m}$ applied as shown in Figure (10). The beam has fixed support at left end and unrestrained along its span except at the fork support which prevents the beam cross section from torsional rotation and moving laterally but allows for the warping deformation.

The geometric properties of the beam section are listed in Table (6). To assess the accuracy and efficiency of the present finite beam element formulation, the quasi-static response is evaluated under a very low excitation frequency $\Omega \approx 0.01f_{t1} = 0.3248\text{Hz}$ and steady state dynamic response with exciting frequencies $\Omega = 120\text{Hz}$, where the first natural torsional frequency of the given beam is $f_{1t} = 32.48\text{Hz}$.

Table 6: Geometric and properties of thin-walled I-section beam.

Parameter	Value	Parameter	Value
E	$200.0 \times 10^9 \text{ N/m}^2$	G	$78.0 \times 10^9 \text{ N/m}^2$
A	7389 mm^2	ρ	8000 kg/m^3
I_{yy}	$86.98 \times 10^6 \text{ mm}^2$	J	$373.7 \times 10^3 \text{ mm}^4$
I_{yy}	$18.82 \times 10^6 \text{ mm}^2$	C_w	$267.7 \times 10^9 \text{ mm}^6$

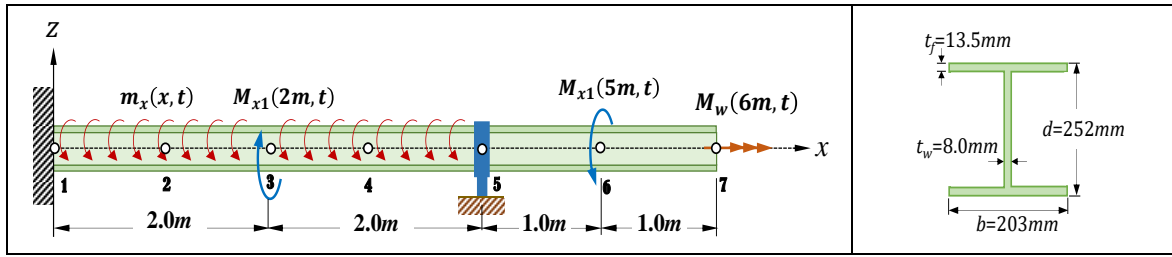


Figure 10: A thin-walled I-beam under various twisting and warping moments.

For validation purposes, the nodal static and dynamic results obtained from the finite element solution (FES) developed in this study are compared with those from the well-established Abaqus model using the B31OS beam element. In the Abaqus simulation, 180 B31OS beam elements are employed, resulting in a total of 1,267 degrees of freedom (DOF) to minimize mesh discretization errors and ensure high accuracy. In contrast, the present finite beam element formulation requires only six beam elements along the beam span, involving just 14 DOF in total.

Static Response Analysis

The quasi-static torsional warping response of the given thin-walled beam is evaluated using two distinct finite element approaches: the present formulation, which utilizes only 14 degrees of freedom (DOF), and the Abaqus finite beam element model, which employs 1,267 DOF. The static results for the nodal torsional rotation angle θ_n and the warping deformation function Φ_n (for $n = 1, 2, 3, \dots, 7$) are presented in Figure 11. These results, derived from both the present formulation and the Abaqus B31OS beam model, are superimposed on the same plots for direct comparison. As shown in Figure 8, there is excellent agreement between the results of the present model using just six beam elements (14 DOF) and those of the Abaqus model using 180 elements (1,267 DOF). This clearly demonstrates that the present finite element formulation can achieve high accuracy with a significantly reduced number of degrees of freedom. Additionally, this indicates that the present finite element solution effectively determines the eigenfrequencies of the given beams.

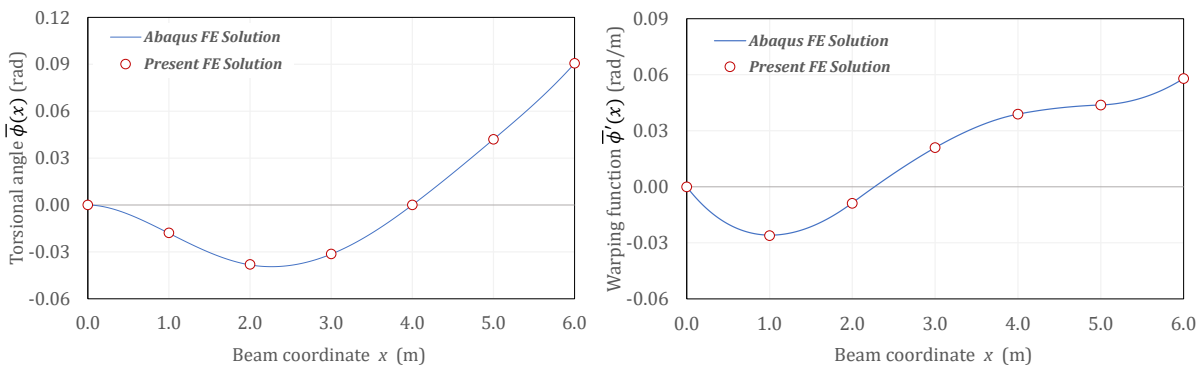


Figure 11: Static torsional analysis of thin-walled I-beam under various twisting and warping moments .

Dynamic Torsional-Warping Response Analysis

The dynamic torsional warping response for the given beam subjected to various twisting and warping moments under exciting frequency ($f = 120\text{Hz}$) are presented in Figure (12). The nodal torsional rotation θ_n and warping deformation Φ_n (for $n=1,2,3,\dots,7$) obtained from the present finite element formulation, which is based on exact shape functions, are compared with the results from the Abaqus finite beam model. The comparison reveals that the present formulation, utilizing only six beam elements and 14 degrees of freedom, shows excellent agreement with the Abaqus model, despite the latter using a significantly higher number of elements (i.e., 180 B31OS elements with 1,267 dof). This leads to conclude that, the computational efforts in the present finite element solutions are several orders of magnitudes less than that of Abaqus beam model solution. This naturally results from the fact that the present finite element formulation is based on the shape functions, which exactly satisfy the homogeneous form of the dynamic governing torsional equation, which in turn eliminates discretization errors encountered in finite element formulation.

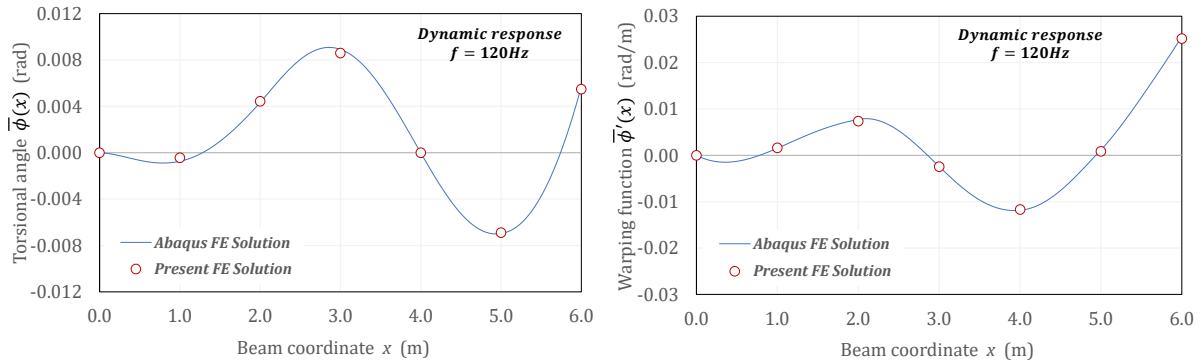


Figure 12: Dynamic torsional analysis of thin-walled I-beam under various twisting and warping moments having exciting frequency $f = 120\text{Hz}$

Summary and Conclusion

Based on the results obtained in this study, the following concluding remarks can be drawn:

1. The governing field equation for the torsional-warping response and related boundary conditions for open thin-walled Vlasov beams under harmonic torsional excitations is derived through Hamilton variational principle.
2. The exact solution for the steady-state torsional response of thin-walled beams, developed in this study, has been effectively utilized to construct a set of exact shape functions that precisely satisfy the homogeneous form of the governing torsional equation.
3. The exact shape functions are used to formulate an efficient finite beam element for torsional-warping response.
4. An efficient and accurate finite beam element has been developed for open thin-walled beams with doubly symmetric cross-sections, featuring two nodes and four degrees of freedom per element. This element is capable of accurately capturing the response under various harmonic torsional and warping moment loadings.
5. The present finite element solution is based on Vlasov beam theory, which neglects shear deformation effects but incorporates warping deformation caused by non-uniform torsion.
6. The beam element eliminates discretization errors associated with other interpolation schemes and delivers highly accurate results with a significantly reduced number of degrees of freedom.
7. The present finite element formulation effectively captures both quasi-static and steady-state torsional responses of open thin-walled beams under harmonic torsional moments.
8. It also successfully predicts the eigenfrequencies and eigenmodes from the steady-state torsional response.
9. The proposed finite element formulation demonstrates excellent agreement with Galerkin and Abaqus beam elements while requiring considerably less computational and modeling effort.

References

- [1] Vlasov, V. Z. (1961), Thin-walled elastic beams, second edition, Jerusalem-Israel Program for Scientific Transactions.
- [2] Seaburg, P.A., and Carter, C.J., (1997), Torsional analysis of structural steel members, American Institute of Steel Construction (AISC), Chicago.
- [3] Kameswara, R., Gupta, B. and Rao, D., (1974), Torsional vibrations of thin-walled beams on continuous elastic foundation using finite element method. Proceedings of International Conference on Finite Element Methods in Engineering, Coimbatore, 231-248.
- [4] Chen, X. and Tamma, K. (1994), Dynamic response of elastic thin-walled structures influenced by coupling effects, Computers and Structures, 51(1): 91-105.
- [5] Aminbaghai M, et al., (2017), Second-order torsional warping theory considering the secondary torsion-moment deformation-effect, Engineering Structures 147: 724–739.
- [6] Mei, C. (1970), Coupled vibrations of thin-walled beams of open section using the finite element method, International Journal of Mechanical Science, 12(10): 883–891.
- [7] Hu, Y, et al., (1996), A finite element model for static and dynamic analysis of thin-walled beams with asymmetric cross-sections, Computers and Structures, 61(5): 897–908.
- [8] Mohareb, M. and Nowzartash, F., (2002), Exact finite element for non-uniform torsion of open sections, Journal of Structural Engineering, 129(2): 215-223.

- [9] Hjaji, M. A. and Mohareb, M. (2013), Harmonic response of doubly symmetric thin-walled members based on the Vlasov theory, II-Finite element solution, CSCE, 3rd Specialty Conference on Engineering Mechanics and Materials, Montreal, Canada.
- [10] Hjaji, M. A., Nagiar, H. M., Allaboudi, E. G. and Krer, M. M. (2021), Exact finite beam element for open thin walled doubly symmetric members under torsional and warping moments, *Journal of Structural Engineering and Applied Mechanics*, 4(4): 267-281.
- [11] Hjaji, Mohammed A. and Mohareb, M. (2014), Coupled Flexural-Torsional Response of Harmonically Excited Monosymmetric Thin-walled Vlasov Beams – II. Finite Element Solution, CSCE, 4th International Structural Specialty Conference, Halifax, Canada.
- [12] Mohammed A. Hjaji, Hasan M. Nagiar, Muftah M. Krer, and Ezedine G. Allaboudi, An Efficient Finite Element of Torsional Dynamic Analysis for Open Thin-Walled Beams Under Torsional Excitations, *Journal of Engineering Research*, University of *Tripoli*, Libya, 34, p17-44, 2022.